



# Distribution and source assignments of polycyclic aromatic and aliphatic hydrocarbons in sediments and biota of the Lafayette River, VA

Nathaniel Maynard<sup>1</sup> · H. Rodger Harvey<sup>1</sup>

Received: 16 August 2022 / Accepted: 22 January 2023 / Published online: 6 February 2023  
© The Author(s), under exclusive licence to Springer-Verlag GmbH Germany, part of Springer Nature 2023

## Abstract

The Lafayette River comprises a tidal sub-estuary constrained by an urban watershed that is bounded by residential areas at its upper reaches and port activity at its mouth. We determined the concentrations and distributions of polycyclic aromatic hydrocarbons (PAHs) and aliphatic *n*-alkanes across 19 sites from headwaters to river mouth in surface sediments (0–2 cm). Potential atmospheric sources were investigated through the analysis of wet and dry deposition samples and intact coals from a major export terminal nearby. The potential consequences for human consumption were examined through analysis of native oyster (*Crassostrea virginica*) and blue crab tissues (*Callinectes sapidus*). A suite of up to 66 parent and alkyl-substituted PAHs were detected in Lafayette sediments with total concentrations ranging from 0.75 to 39.00  $\mu\text{g g}^{-1}$  dry wt. Concentrations of aliphatic *n*-alkanes (*n*-C<sub>16</sub> – *n*-C<sub>31</sub>) ranged from 4.94 to 40.83  $\mu\text{g g}^{-1}$  dry wt. Source assignment using diagnostic ratios and multivariate source analysis suggests multiple sources contribute to the hydrocarbon signature in this metropolitan system with automotive and atmospheric transport of coal dust as the major contributors. Oyster tissues showed similar trends as PAHs observed in sediments indicating similar sources to water column particles which ultimately accumulate in sediments with crabs showing altered distributions as a consequence of metabolism.

**Keywords** Estuary · PAHs · Hydrocarbons · Atmospheric Deposition · Sediments · Coal

## Introduction

The Lafayette River is a 10-km-long tidal estuary bounded by largely residential areas at its upper reaches and port activities at its confluence with the Elizabeth River. Although eventually connected to the lower Chesapeake Bay, the Lafayette system is unique as the 43.28 km<sup>2</sup> watershed is entirely contained within metropolitan Norfolk, VA (Egerton et al. 2014). It is bounded by over 1000 waterfront homes and occupied by over 40% of the city residents (VA Dept. of Health 2012; Egerton et al. 2014). The restricted exchange with the Elizabeth River, dense residential housing (over 45% of total land use), and limited light industry

(8%) makes the Lafayette River an urban watershed largely driven by freshwater inputs through precipitation and localized drainage (Egerton et al. 2014; Mulholland et al. 2018; Macias-Tapia et al. 2021). As with many urban rivers, local stormwater runoff can lead to the introduction of a variety of contaminants (e.g., Masoner et al. 2019). The major control on water exchange of the Lafayette River is tidal events which cause regular mixing of the system with a rather long residence time of 1 to 4 months (White 1972).

The consequences of runoff into the Lafayette River have been linked to the introduction of contaminants and various nutrients which are reflected in regular algal blooms (Mulholland et al. 2018). The Lafayette watershed also experiences regular tidal flooding as much of the surrounding land's elevation is less than 5 m above sea level (Kleinosky et al. 2007). With regular tidal mixing, the Lafayette experiences a largely brackish salinity regime; however, the river also sees large swings in salinity ranging from 8 to 22 driven by rainfall as the system is a major corridor for surface water drainage from residential streets (Egerton et al. 2014). In recent years, several restoration efforts to improve the river

Responsible Editor: Philippe Garrigues

✉ Nathaniel Maynard  
nmayn002@odu.edu

<sup>1</sup> Marine Organic Geochemistry and Ecology Lab,  
Department of Ocean and Earth Sciences, Old Dominion  
University, Norfolk, VA 23529, USA

have been implemented including living shorelines, rain gardens to capture rainfall runoff, and 80 acres of oyster reef to improve water quality and revitalize the river (NOAA 2020).

With the varied activities for the Lafayette River, some inputs of organic contaminants are expected from both anthropogenic and natural sources. Historic analysis has been limited to specific industrial sites of major concern and the linked Chesapeake Bay despite the significant residential population and multiple recreational uses for the river (Dickhut et al. 2000; Walker and Dickhut 2001; Kimbrough and Dickhut 2006). In addition, within 3 km of the river mouth lies a major rail export terminal for east coast coal (Lamberts Point Coal Terminal). With an estimated export of over 28 Mt year<sup>-1</sup>, it is one of the largest coal terminals in the USA (Bounds and Johannesson 2007). The heart of the terminal is Pier 6 which relies on open air transfer of coal from rail cars. In 2000, it was estimated that the coal terminal released 35 tons of airborne particulate coal during loading; thin layers of probable coal dust are typically observed in the nearby residential neighborhood (Bounds and Johannesson 2007).

Polycyclic aromatic hydrocarbons (PAHs) and normal-alkanes (*n*-alkanes) are two important contaminants of concern for the Lafayette River sub-estuary and were examined for this study. PAHs are of environmental concern due to their well-established immunotoxicity, genotoxicity, carcinogenicity, and reproductive toxicity (Qiao et al. 2006). In the past, PAHs, along with various bioassays, have been utilized to characterize sediment quality in estuaries (Rizzi et al. 2017). Sources of PAHs can be either natural or anthropogenic derived with the natural sources coming from terrestrial debris or oil seepage (e.g., Harvey et al. 2014). Anthropogenic sources of PAHs are most often categorized as either petrogenic or pyrogenic in origin (Pies et al. 2008; Saha et al. 2009; Masood et al. 2016). Petrogenic PAHs originate from fossil fuels and tend to be introduced into the system through discharges, accidental spillage, or urban runoff (Masood et al. 2016). For this study, a number of petrogenic PAH sources common in urban areas were targeted and included those derived from used motor oil (Wang et al. 2000 and Boonyatumanond et al. 2007), tire particles (Boonyatumanond et al. 2007) asphalt (Boonyatumanond et al. 2007), and lump coal particles. The second group to be considered is pyrogenic PAHs which are typically formed under high-temperature combustion and/or pyrolysis of fossil fuels or organic matter (Masood et al. 2016). These pyrogenic PAH sources included those associated with residential heating (Li et al. 2003), coal combustion (Li et al. 2003), diesel vehicle particulate emissions (Li et al. 2003), gasoline vehicle particulate emissions (Li et al. 2003), fuel–oil combustion particles (Li et al. 1999), pine-wood soot particles (Schauer et al. 2001), and coal-tar sealants (Mahler et al. 2005). Once introduced into the aquatic system, all PAHs tend to accumulate in underlying sediments due to

their hydrophobicity and strong affinity for organic matter (Yim et al. 2005). To assign PAH sources, several methods are commonly utilized including PAH diagnostic ratios and multivariate analysis (Sofowote et al. 2008). For sediments in particular, PAH source assignments are often complicated by structural modification or degradation from their original sources which alter their distribution (Neff et al. 2005; Norris and Henry 2019; Davis et al. 2019). The hydrophobicity of the PAHs also often leads to their bioaccumulation in animal tissue which can be of concern to individuals consuming contaminated food.

Aliphatic *n*-alkanes also have multiple natural or anthropogenic sources (Nemr et al. 2016). Natural sources of *n*-alkanes include terrestrial plant waxes, marine phytoplankton, biomass combustion, and natural oil seeps (Tolosa et al. 2004). Specific long- and odd-chain *n*-alkanes are largely considered indicative of higher plant material while short- and even-chain *n*-alkanes reflect petroleum sources (e.g., Wang et al. 2006; Harvey et al. 2014). These *n*-alkanes also adsorb readily to sediments and tend to accumulate over time.

A complication for any PAH source assessment is the impact of weathering reactions during transport to the eventual matrix sampled (Abdel-Shafy and Mansour 2016). Several factors that can selectively alter various PAHs include biodegradation, photooxidation, chemical oxidation, and the consumers metabolism (Kim et al. 2007; Korfmacher et al. 1980; Javier Rivas 2006; Livingstone 1998). Biodegradation of PAHs appears to occur principally in the dissolved or vapor phase, with limited loss once adsorbed to soil particles (Chauhan et al. 2008). This leads to changes in degradation rate and distribution which are often dependent upon desorption rates of PAHs from soil particles (Hatzinger and Alexander 1995). Photooxidation is another important weathering process for particles in the vapor and aqueous phase and also is more effective on LMW PAHs (Korfmacher et al. 1980). Chemical degradation is generally thought to play a very limited role in PAH degradation (Javier Rivas 2006). Metabolism by vertebrate and invertebrate species can alter PAHs via Phase I and Phase II biotransformation enzymes (Livingstone 1998). Relevant to the current work is that these enzymes tend to be in the highest concentrations in the hepatopancreas of blue crabs and thus it is important to sample hepatopancreas tissue separately from muscle tissue (Mothershead II et al. 1991; Livingstone 1998). Of the two invertebrates investigated in this study, crustaceans appear to metabolize aliphatic and aromatic hydrocarbons at about three times the rate of mollusks based on wet tissue and comparable concentrations (Livingstone 1998).

The goal of this study was a comprehensive examination of PAH and *n*-alkane concentrations in the Lafayette River system and its major source contributors. This included the estimation of atmospheric source imprints to

this metropolitan tributary. Although the Environmental Protection Agency (EPA) has targeted 16 PAHs as priority pollutants (Qiao et al. 2006), the analysis here examined the full suite of 66 PAHs present to capture the breadth of potential sources entering the river and sequestered in sediments. In addition, the analysis included targeted analysis of benthic residents as oyster and blue crab tissues to examine the burdens of PAHs on Lafayette River biota with potential links to human consumption. The information gained allows assessment of the current status of the Lafayette system and information for future evaluation of ongoing restoration projects.

## Materials and methods

### Sample collection

The Lafayette River is a shallow and dynamic tidal estuary with a mean depth of 1.3 m; the central channel has a maximum depth of 7.6 m (Blair et al. 1976). Regular maintenance dredging is not conducted on this system with the

last event in 1993 on the federally maintained channel from the outflow connection with the Elizabeth River to Hampton Boulevard Bridge (The City of Norfolk 2013). Land use of the area surrounding the Lafayette River is 58% residential/recreational, 14% roads/parking lots, 8% institutional, and 12% industrial/commercial (Macias-Tapia et al. 2021). This study collected samples from multiple locations within the Lafayette watershed including surface sediments, wet and dry atmospheric deposition samples, animal tissues, and coals (see Fig. 1 and supplemental table S1).

### Sediment and tissue samples

Surface sediments (0–2 cm) were collected across 19 sites including several headwater branches of the Lafayette River to its confluence with the Elizabeth River in June 2014 (Fig. 1). In 2015, surface sediment was also collected from Golf Course Inlet (GCI), Lambert's Point Inlet (LPI), and Storm Overflow (SO). In 2021, additional sediment was collected from site 2 to gauge the impact of recent restoration efforts. All sediment samples were obtained using a precleaned hand-held coring device, except for sites 16a

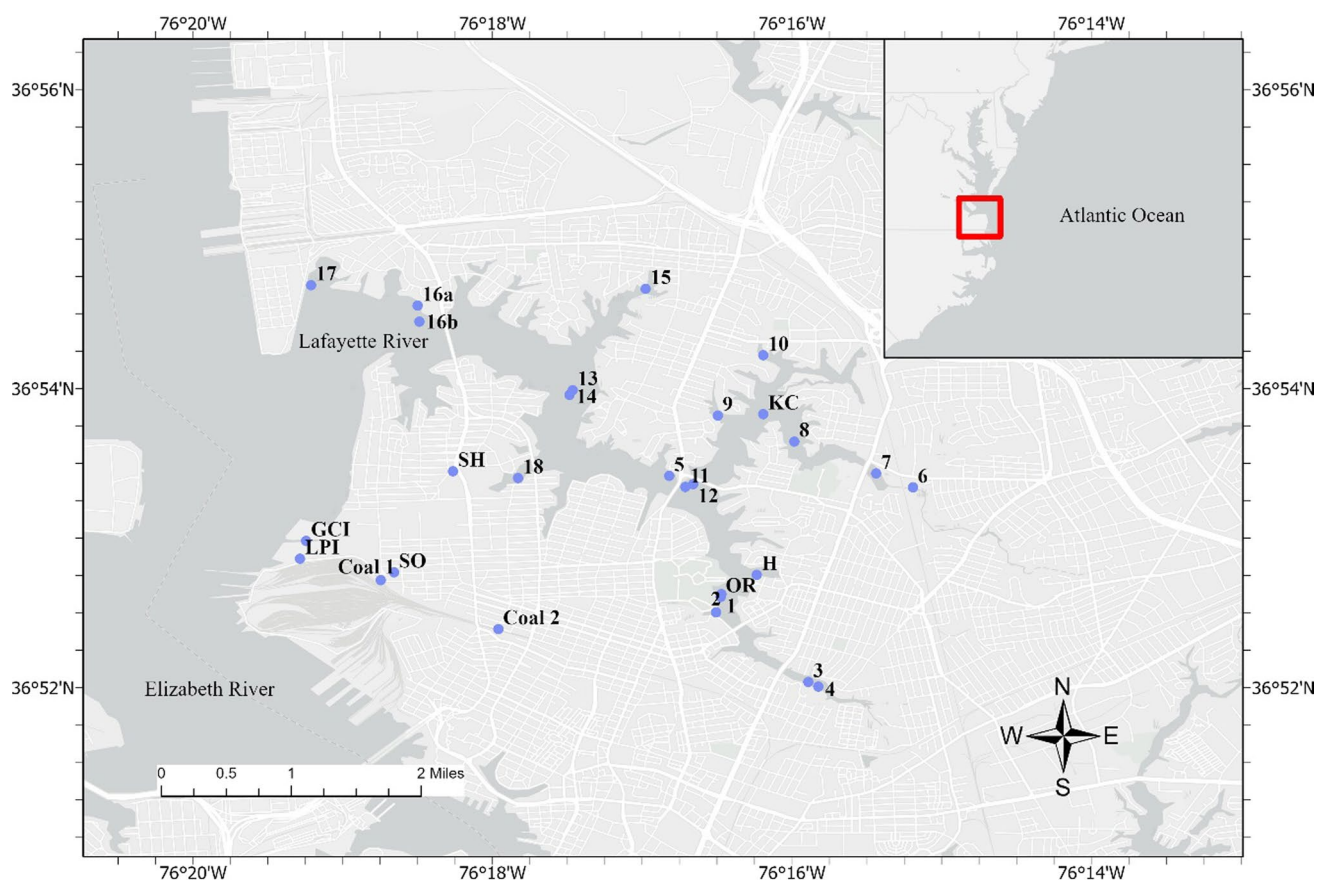


**Fig. 1** Map of station locations sampled during 2014, 2015, and 2021 for aromatic and aliphatic hydrocarbons. Sample details for each site are described in supplemental table S1. Base layer provided through VGIN, Esri, HERE, Garmin, SafeGraph, GeoTechnologies, Inc

and 16b which required a sediment grab due to the depth of water. Overlying water was siphoned off and the top 2 cm of sediment was removed for chemical analysis. The samples were stored in precleaned plastic I-Chem jars with Teflon-lined screw caps and immediately frozen at  $-80\text{ }^{\circ}\text{C}$  until analysis.

Atlantic blue crabs were collected adjacent to sediment sites at two locations (KC and H sites) in July 2014 (Fig. 1). Following collection, the crabs were placed in the freezer to be euthanized and then were refrigerated for 2 h prior to dissection with sterile and solvent-washed tools. Muscle tissue from the claws and back fins from animals at each collection site were combined. The hepatopancreas was also dissected and the tissue separated for each collection site.

Adult oysters were collected by hand in October 2021 from an existing oyster reef (Fig. 1). Once back in the laboratory, oysters were rinsed to remove external material from shells and immediately dissected. All gut material was removed from the oyster tissue with filtered Nanopure water. Tissue samples were placed in a precleaned plastic I-Chem jar with a Teflon-lined screw cap and frozen at  $-80\text{ }^{\circ}\text{C}$ .

### Air deposition and coal samples

Wet and dry deposition samples were collected using a standard Aerochem Metrics Model 301 atmospheric sampler (areal opening of  $20.25\text{ cm}^2$ ) mounted on the rooftop of an academic building (SH) on the ODU campus away from nearby inputs to get representative samples for material deposited to the nearby Lafayette River (see Fig. 1). Wet deposition samples were collected into precleaned glass bottles with collection times following major rain events over 1 month. Rain samples were subsequently filtered through combusted  $0.7\text{-}\mu\text{m}$  GF/F filters for retention of particles for analysis. A parallel dry deposition sample was collected over a 1-week dry period at the end of the 4-week sampling using the same sample bucket but no precipitation. Particles in the dry deposition vessel were concentrated by wiping with multiple combusted  $0.7\text{-}\mu\text{m}$  GF/F filters dampened with methanol:Nanopure  $\text{H}_2\text{O}$  (1:1 v/v). The filters were folded and placed in pre-combusted foil and frozen at  $-80\text{ }^{\circ}\text{C}$  until extraction.

Randomized pieces of coal adjacent to the Lambert's point shipping terminal were obtained by collection of fragments (Fig. 1). Coals were rinsed with Nanopure water, ground with a precleaned mortar and pestle, and stored in precleaned plastic I-Chem jars with Teflon-lined screw caps until extraction.

### Sediment carbon and nitrogen

Sediment total organic carbon (TOC) was determined using an Exeter Analytical 440-XA Elemental Analyzer using

standard combustion protocols (EPA method 440; Zimmerman et al. 1997). Lyophilized sediments were first treated to remove carbonates with 1N HCl and stirring using a glass rod. After acid treatment, sediments were left in vials uncapped at room temperature for 1 h and then dried overnight at  $60\text{ }^{\circ}\text{C}$  before analysis. Analytical precision of repeated analysis was  $\pm 3\%$ .

## Analysis of hydrocarbons

### Extraction, purification, and GC/MS analysis

Analysis of aromatic and aliphatic hydrocarbons followed the approach of Harvey et al. (2014) with minor modifications. All sediment and coal samples were first lyophilized and homogenized prior to chemical analysis. Tissue samples were lyophilized and cut into small pieces prior to extraction using solvent-washed stainless steel scissors. Wet atmospheric deposition particles were filtered onto combusted  $0.7\text{-}\mu\text{m}$  GF/F filters. All samples (ranging from 0.59 to 5.38 g) were transferred into Green Chem glass vessels containing a mixture of hexane: acetone (1:1 v/v, 30 mL) (refinement of EPA Method 3546). Five perdeuterated reference compounds were added (acenaphthene- $\text{d}_{10}$ , phenanthrene- $\text{d}_{10}$ , benz[a]anthracene- $\text{d}_{12}$ , benzo[a]pyrene- $\text{d}_{12}$ , and benzo[g,h,i]perylene- $\text{d}_{12}$ ) as internal surrogates for quantification of PAHs (refinement of EPA Method 8270). *n*-Octadecane- $\text{d}_{38}$  was also added as an internal surrogate for samples where *n*-alkanes were quantified. Samples were extracted ( $80\text{ }^{\circ}\text{C}$  for 30 min) using a MARS microwave accelerated extraction system (CEM Corp., Matthews, NC). The total extracts were allowed to cool before being filtered through pre-cleaned and combusted glass wool into round-bottom flasks. The Green Chem glass vessels were rinsed twice with a hexane:acetone (1:1 v/v) mixture and combined with the extracts. The total extracts were concentrated using rotary evaporation. The total extracts were split into vials prior to analysis.

Solid phase extraction (SPE) was performed on the total lipid extracts of sediment and tissue samples to isolate hydrocarbons from polar materials using Strata SI-1 Silica ( $55\text{ }\mu\text{m}$ , 70A) Teflon-coated SPE columns (500 mg 3 mL, Phenomenex). Columns were conditioned with dichloromethane:methanol (2:1 v/v) and hexane was used as the elution solvent. The eluted hydrocarbon fractions were concentrated using nitrogen gas and transferred to 4-mL amber vials using known volumes of hexane to bring internal surrogate concentrations near  $2\text{ ng }\mu\text{L}^{-1}$ . Identification of PAHs was carried out by capillary gas chromatography (GC) with an Agilent 7890A system coupled to an Agilent 5975C Network Mass Selective Detector (MS) in electron ionization mode. A J&W Scientific DB-5MS fused silica column ( $60\text{ m}$ ,  $0.320\text{ mm}$  id,  $0.25\text{ }\mu\text{m}$  film thickness) was used and the GC/MS was operated in selected ion monitoring (SIM)

mode. Samples were injected in splitless mode at an initial oven temperature of 50 °C and an injector temperature of 250 °C with helium as the carrier gas. The oven temperature was ramped at 15 °C min<sup>-1</sup> to 120 °C and then 3 °C min<sup>-1</sup> to 300 °C before holding at 300 °C for 10 min. To quantify PAH concentrations, the base peak area for individual PAH compounds was adjusted relative to the known amount of one of the five internal surrogates added based on rings and functional groups (refinement of EPA Method 8270D).

For a subset of samples, aliphatic *n*-alkanes were quantified using similar conditions as for PAH's samples. Capillary GC using an Agilent 7890A Network GC system with flame ionization detection (GC-FID) was used with the GC column and temperature program similar to that for the PAH analysis. The base peak area of individual *n*-alkanes was adjusted relative to the known concentration of the perdeuterated internal surrogates added (*n*-Octadecane-d<sub>38</sub>). Full-scan mode by GC-MS was used for identification.

### Quality assurance and quality control

All glassware used for sample processing and analysis was pre-cleaned, combusted at 450 °C for 4 h, and subsequently rinsed with solvent before use. Procedural blanks were processed in parallel with all sets of field samples and followed the identical protocol. For atmospheric deposition samples, blanks also included GF/F filters spiked with internal surrogates to evaluate retention and recovery. All internal surrogates were added prior to processing of samples and integrated peak areas were used to calculate initial concentrations. Procedural blanks were also used to evaluate the contamination of the samples once in the laboratory setting. A sediment reference (NIST standard reference material 1944) with certified PAH values was analyzed in parallel to evaluate the accuracy of analysis and estimate recovery from sediment matrices. Total PAH concentration obtained from the SRM resulted in 114.45% of the expected concentration; sediment samples were not corrected for the small difference. Procedural blanks were < 6% of the PAH concentrations observed and < 12% of the *n*-alkane concentrations, respectively. A calibration curve generated using the internal standard solution determined a lower detection limit of 0.1 ng for individual PAHs.

### Statistical analyses

Principal component analysis (PCA) was preformed utilizing MATLAB to examine correspondence of individual PAHs among samples using relative abundance normalized to dry weight for all the locations sampled with various source distributions. The PCA loading score results described individual PAH contribution to the variance explained by each principal component (PC). Varimax rotation was used to

cluster the loading values around 1 and 0 for interpretation (Sofowote et al. 2008). All concentrations below the lower limits of detection were set to a relative abundance value of 0.1% for PCA analysis to account for statistical significance. The goal of the PCA was to use the broad suite of PAHs quantified to compare distribution patterns and decipher potential sources of PAHs based on both local sources and documented literature values. Comparison of specific PAH ratios was also used to identify potential sources of hydrocarbons to the system.

## Results

### Concentration and distribution of PAHs and alkanes across sites and matrices

#### PAHs and alkanes in sediments

Up to 66 PAHs were detected in Lafayette River surface sediments across several field years (Fig. 2). Total sediment PAH concentrations ranged from 0.75 µg g<sup>-1</sup> dry wt. at station 14 in the central river channel to 52.39 µg g<sup>-1</sup> dry wt. at LPI station closest to the Norfolk coal terminal. For site 2 resampled in 2021, the total PAH surface sediment concentration declined to 8.79 µg g<sup>-1</sup> dry wt. from the initial value of 39.00 µg g<sup>-1</sup> dry wt. in 2014. The relative distribution of PAHs in Lafayette sediments was similar across sites for much of the system while differences were observed at sites located outside of the Lafayette River including LPI, GCI, and SO. For Lafayette sediments, high molecular weight (HMW) PAHs (> 3 rings) were generally favored, accounting for 67.9–91.2% of the total concentration. The highest concentrations in sediments were observed for fluoranthene (Fl), pyrene (Pyr), and benzo[b]fluoranthene (Bbf). For all sediment samples collected, parent PAHs were prominent, accounting for 72.8–90.8% of total PAHs. Water depth at the collection sites did influence the total concentrations observed with the deeper stations (1 to 6 m) in the central channel having lower total PAH concentrations than shallow stations (< 1 m) near shore (see supplemental table S1). A Wilcoxon rank-sum test was utilized as the data was not normally distributed and confirmed that deeper stations were significantly lower in concentration ( $p < 0.05$ ). There was also a strong correlation ( $r = 0.8875$ ,  $p < 0.05$ ) between elevated TOC in sediments (0.88–9.32%) and increased PAH concentrations (as dry weight) across the sites (see supplemental table S1). While PAH concentrations normalized to dry weight are summarized here, individual PAH concentrations are detailed in supplemental table S2 (A), (B), (C), and (D) including sediment concentrations normalized to TOC.

Aliphatic *n*-alkanes (*n*-C13 to *n*-C33) in sediments varied almost tenfold in total concentrations across the sites

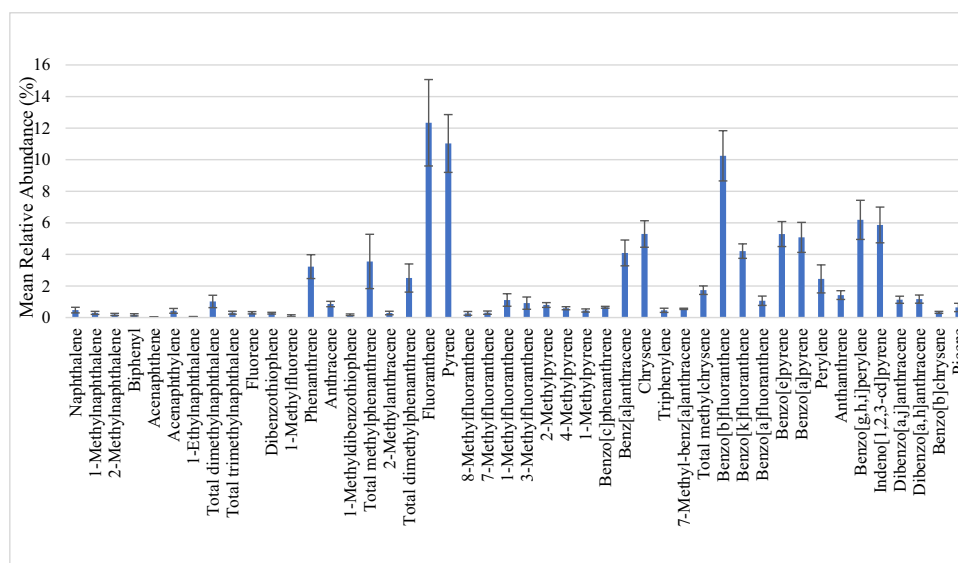


**Fig. 2** The mean relative abundance ( $\pm 1$  SD) of PAHs observed in surface sediment across 19 sites spanning the Lafayette River system. PAH distributions were consistent across sights with the PAHs in highest abundance including Fl, Pyr, and Bbf. Several PAH isomers have been aggregated to simplify illustration of the 66 structures quantified. Total dimethylnaphthalenes include  $\Sigma$ 1,3-, 2,7-, 1,6-, 1,5-, 1,4-, and 2,3- isomers. Total trimethylnaphthalenes include  $\Sigma$ 1,6,7-,

2,3,6-, 1,4,6-, and 1,4,5- isomers. Total methylphenanthrenes include  $\Sigma$ 1-, 2-, 3-, and 9- isomers. Total dimethylphenanthrenes include  $\Sigma$ 3,5-, 2,6-, 2,7-, 3,9-, 1,6-, 1,7-, 4,9-, 1,9-, 1,8-, and 1,2- isomers. Total methylchrysenes include  $\Sigma$ 1-, 2-, and 3- isomers. Concentrations of individual isomers across all sediments are described in supplemental table S2 (A), (B), (C), and (D)

( $4.68 \mu\text{g g}^{-1}$  at SO to  $40.83 \mu\text{g g}^{-1}$  dry wt. at station 2) (see supplemental Fig. S8 & S9). Short ( $n\text{-C}_{13} - n\text{-C}_{22}$ ) vs. long chain ( $n\text{-C}_{23} - n\text{-C}_{33}$ ) comparisons favored long-chain alkanes, with long-chain alkane values accounting for at least 36% and up to 90% of alkanes across all sites. Only four sites favored short-chain alkanes (5, 14, 16a, and LPI). The majority of sites that favored long-chain alkanes also showed a predominance of odd chain lengths ( $n\text{-C}_{23} - n\text{-C}_{33}$ )<sub>odd</sub> ranging from 77 to 87%. As seen for PAHs, water depth was a significant discriminator for total  $n$ -alkane concentrations based on Wilcoxon rank-sum ( $p < 0.05$ ) with higher concentrations of total  $n$ -alkanes found at shallow stations. Results for the  $n$ -alkane concentrations in sediment are specified in supplemental table S4 (A), (B), (C), and (D).

#### PAHs and aliphatic alkanes in airborne particles and coals

Atmospheric deposition and lump coal samples used to constrain potential sources of PAHs observed in sediments contained up to 62 PAHs. Wet deposition samples differed in precipitation amounts and the timing between rain events and resulted in variable PAH concentrations with a mean value of  $98.43 \pm 105.21 \text{ ng L}^{-1}$  rainfall. Collectively, wet deposition samples showed high abundances of naphthalene (Nap), Fl, Pyr, chrysene (Chr), and Bbf, with shifts in PAH distribution across rain events (Fig. 3c).

The dry deposition sample showed a similar total PAH concentration at  $116.06 \text{ ng cm}^{-2}$  but differed because of a strong dominance of HMW PAHs (Fig. 3b). Wet deposition samples showed a varied distributions with some favoring LMW PAHs while others favored HMW PAHs.

For coal samples, total PAH concentrations were very similar between individual samples at  $24.53$  and  $25.50 \mu\text{g g}^{-1}$  dry wt. respectively, and in distribution for both LMW and alkyl-substituted PAHs (Fig. 3a). While lump coals favored LMW PAHs, a comparison of the PAH distribution for the HMW portion of coals mirrored that seen in the dry atmospheric deposition and sediment samples (Fig. 4). The majority of the LMW PAHs were in low abundance for the dry deposition and sediment samples (Figs. 2 and 3b). Individual PAH concentrations for air deposition and coal are described in supplemental table S3 and supplemental table S2(E), respectively.

Aliphatic  $n\text{-C}_{13} - n\text{-C}_{33}$  alkanes were targeted for analysis in air deposition samples. Total concentrations of  $n$ -alkanes ranged from  $1.30 \mu\text{g cm}^{-2}$  in the dry deposition sample to  $17.79 \mu\text{g L}^{-1}$  on July 20th. The distribution of short- vs. long-chain alkanes varied among the samples over time with the first two wet deposition samples and the final dry collection favoring long-chain alkanes while the remaining three wet deposition samples favored short-chain alkanes. The distribution of alkanes showed odd chain lengths were favored and ranged from 69 to 93%.

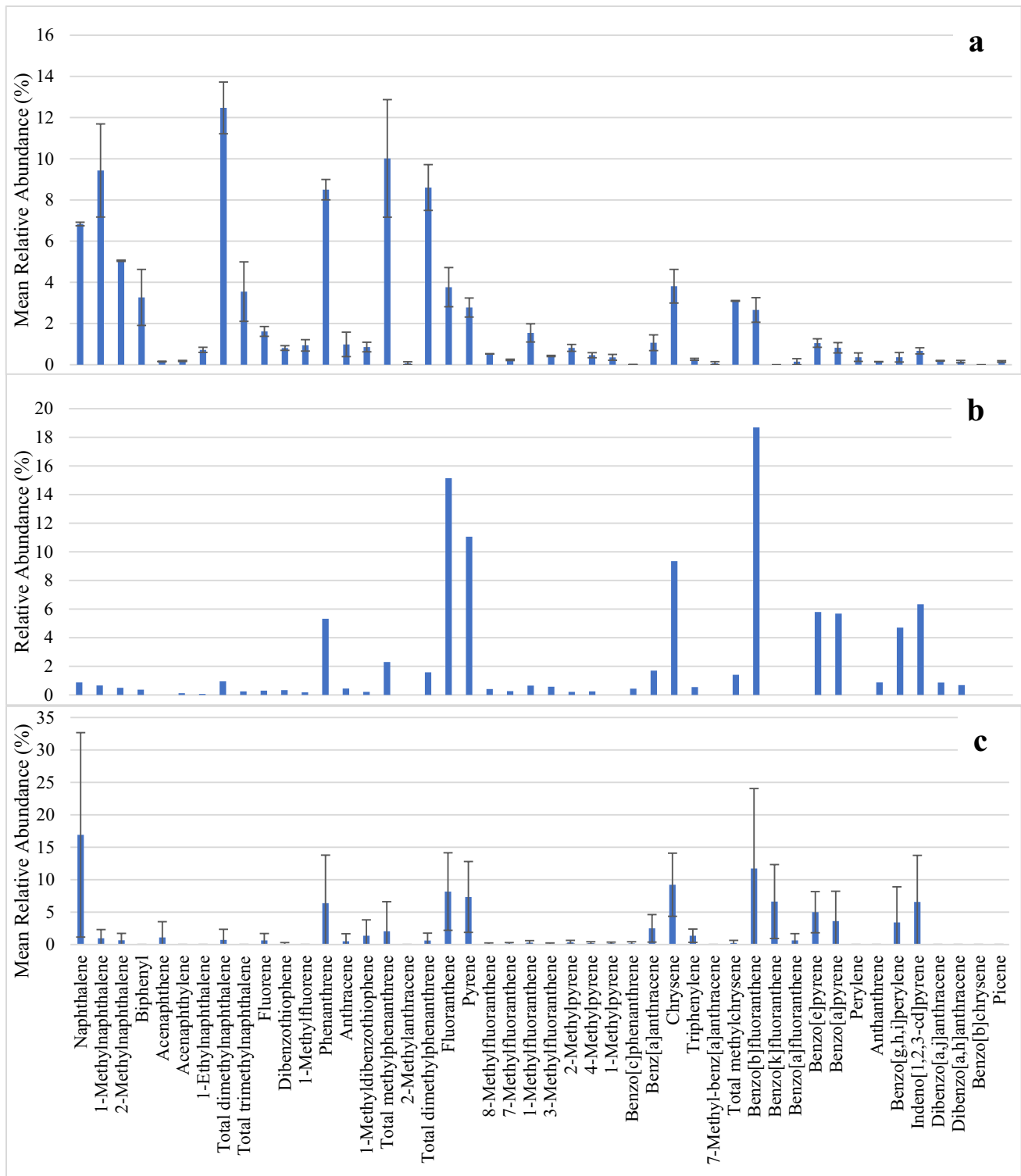
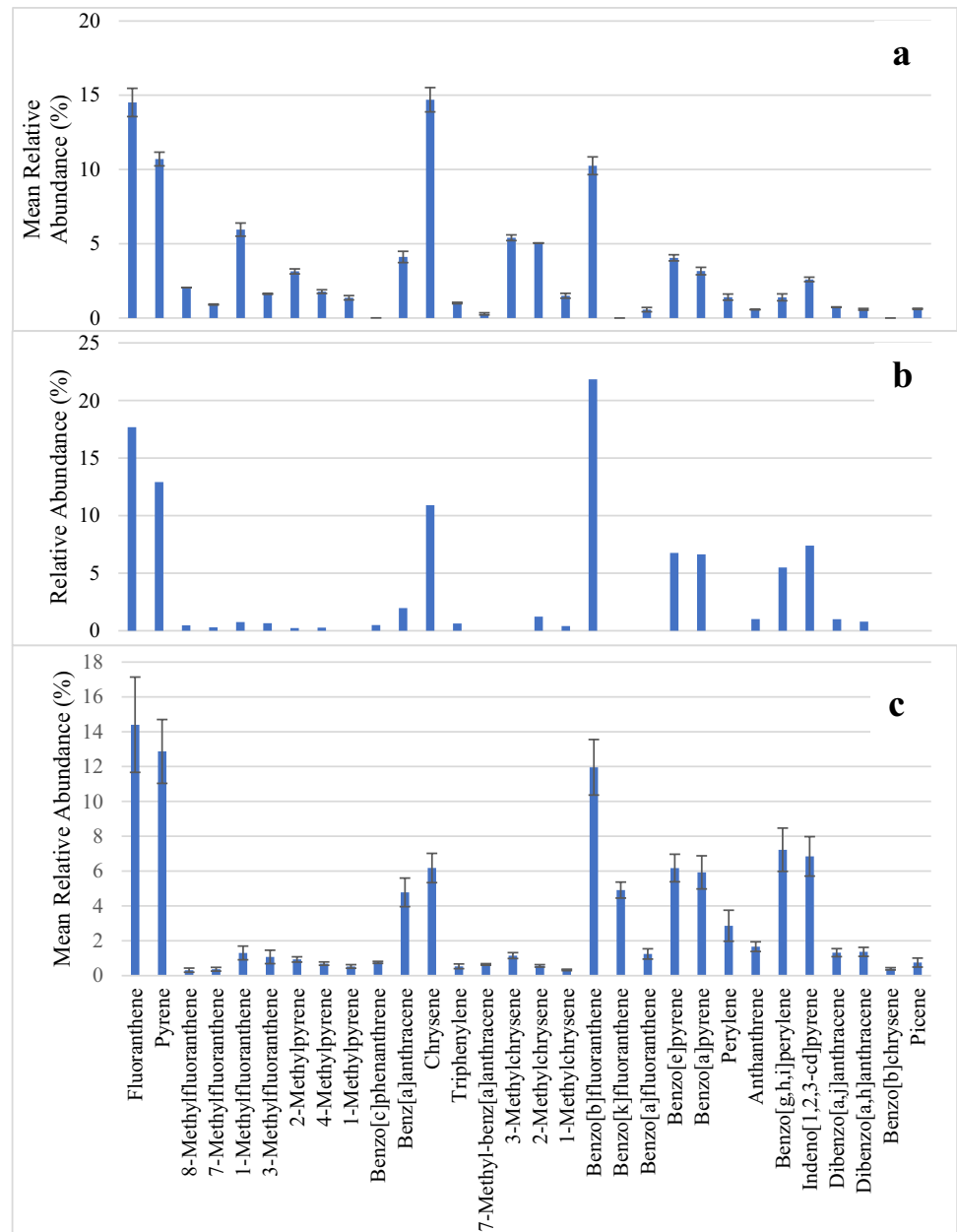


**Fig. 3** The relative abundance of PAHs in (a) intact coal fragments ( $n = 2$ ), (b) a dry atmospheric deposition sample ( $n = 1$ ), and (c) average values ( $\pm 1$  SD) for wet deposition samples ( $n = 5$ ). For illustration, multiple isomers of dimethylnaphthalene, trimethylnaphthalene

methylphenanthrene, dimethylphenanthrene, and methylchrysene have been aggregated as described in Fig. 2. Although wet deposition varied with precipitation, the dry deposition sample shows a predominance of HMW PAHs compared to the LMW PAHs favored in coals

**Fig. 4** The relative abundance of HMW (> 3 rings) PAHs present in (a) coal fragments ( $n=2$ ), (b) a dry atmospheric deposition sample ( $n=1$ ), and (c) Lafayette River surface sediments ( $n=19$ ). In all three matrices, high abundances of Fl, Pyr, Chr, and Bbf were notable



For coals, total concentrations of alkanes ( $n\text{-C}_{13} - n\text{-C}_{33}$ ) ranged from 8.34 to 17.48  $\mu\text{g g}^{-1}$  dry wt. between the two samples. Short-chain alkanes were predominant in both samples (63% and 79%) and both samples showed the majority of  $n$ -alkanes were odd chain length (57–67%). Detailed results for the  $n$ -alkane concentrations in deposition samples and coals are described in supplemental table S5 and supplemental table S4(D).

#### PAHs and aliphatic alkanes in biota tissues

PAH distribution for resident oyster tissues largely reflected nearby sediment distributions, while crab samples differed.

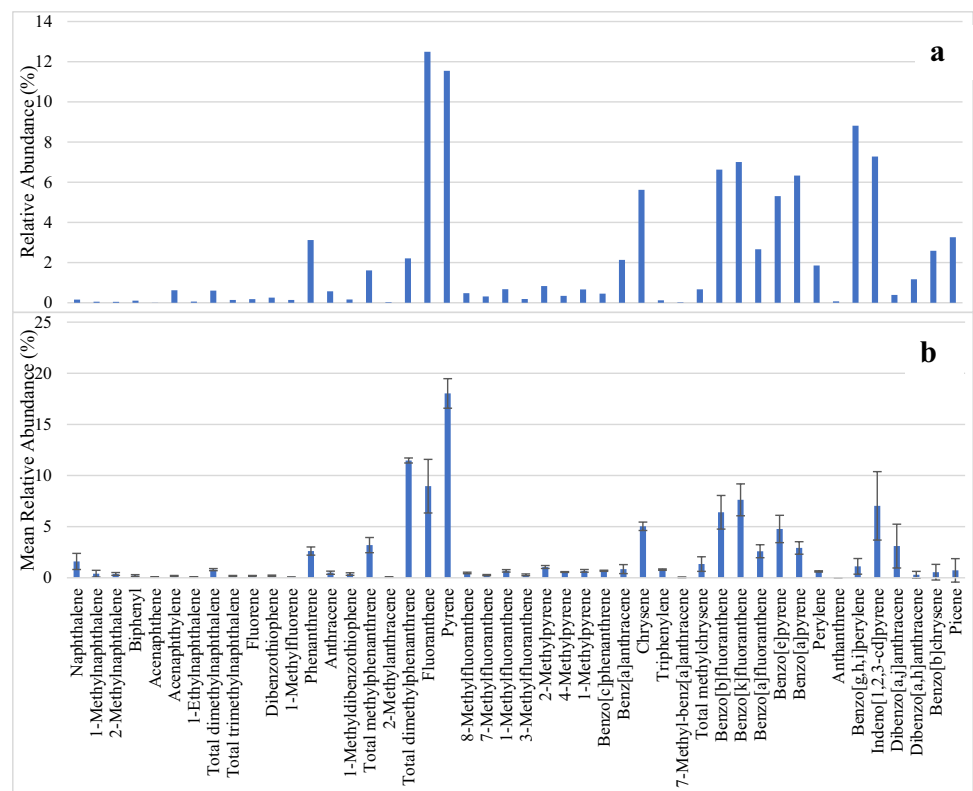
Although up to 65 PAHs were detected in oyster and crab tissues, PAH concentrations differed among tissue types with average values of  $0.18 \pm 0.09 \mu\text{g g}^{-1}$  dry wt. in oysters,  $1.47 \mu\text{g g}^{-1}$  dry wt. in crab hepatopancreas tissue, and  $1.51 \mu\text{g g}^{-1}$  dry wt. in crab muscle tissue. Many of the targeted compounds were below the detection limit in crab tissues. Where observed, tissues were dominated by HMW PAHs, with the exception of crabs at the KC site and suggesting the impact of active metabolism (see Discussion and supplemental table S2 (D) and (E)). With one exception, crab's tissues were also dominated by parent PAHs accounting for 60–86% of the total concentration. There was no significant difference between the hepatopancreas and crab



muscle tissue PAH concentrations. For oysters, age based on shell size showed that more mature oyster had the highest concentration of total PAHs while the smallest oyster had the lowest concentrations despite normalization to tissues dry weight. The distributions of the relative abundance for PAHs in the oyster tissue shows the same trend as the distributions observed in sediment from site 2 resampling which is near the oyster reef (Fig. 5a and b). Individual PAH concentrations in tissue are shown in supplemental table S2 (D) and (E).

Aliphatic *n*-alkanes across 16–31 carbons were observed in crab tissue samples with highest values in hepatopancreas tissue. The average muscle tissue concentration was  $5.41 \mu\text{g g}^{-1}$  dry wt. tissue, and the hepatopancreas tissue average was  $32.62 \mu\text{g g}^{-1}$  dry wt. tissue. Long-chain alkanes were dominant in three of the four crab samples while the hepatopancreas tissue from the KC site contained 47% long-chain alkanes as well. Long-chain alkanes were typically odd except for muscle tissue from the KC site which had 55% of its long-chain alkanes even. Crab tissue *n*-alkane distributions did not reflect surface sediment distributions in proximity to the crab sampling sites. Individual results for the *n*-alkane concentrations in tissues are described in supplemental table S4 (D).

**Fig. 5** The relative abundance of observed PAHs in (a) surface sediment at site 2 resampled in 2021 ( $n=1$ ) compared to (b) oyster tissues collected nearby ( $n=3$ ) ( $\pm 1$  SD). Isomers of dimethylnaphthalene, trimethylnaphthalene, methylphenanthrene, dimethylphenanthrene, and methylchrysene have been aggregated for illustration as described in Fig. 2. Identical PAHs comprise several major components found in both oyster tissue and sediment. Fifty-three of the 66 PAHs investigated were found in all oyster and Lafayette sediment samples



## Discussion

### Hydrocarbons in the Lafayette system

The distributions of PAHs and related *n*-alkanes presented here are the most detailed to date for the Lafayette River sub-estuary and show a system with varied values despite its relatively compact watershed. Although the number of PAHs measured for the Lafayette River compared to similar urbanized estuarine systems differ, this system appears to have lower concentrations compared to other metropolitan systems despite the more comprehensive coverage of PAHs

**Table 1** A comparison of total PAH concentrations observed in Lafayette River sediments and similar estuary, harbor, and bay locations with industrial and residential activity. Values seen in the Lafayette system are generally lower than other metropolitan environments

Location	Range ( $\mu\text{g g}^{-1}$ dry wt.)	References
Bear Creek, USA	12.30–98.40	(Hartzell et al. 2017)
Boston Harbor, USA	7.27–358.09	(Wang et al. 2001)
San Francisco Bay, USA	2.65–27.68	(Pereira et al. 1996)
Elizabeth River, USA	0.73–412.98	(Vogelbein et al. 2008)
Lafayette River, USA	0.75–39.00	This study

(Table 1). The nearby Elizabeth River's southern branch was highly contaminated from the past creosote industry and retains high concentrations of a number of contaminants, but it appears that PAH transport to the Lafayette has been limited. Although preliminary, the resampling at site 2 in 2021 shows a significant decline in PAH concentrations compared to 2014 and suggests for this site that recent restoration efforts have led to a reduction in PAHs. Further analysis will be needed to assess the overall impact of restoration efforts on the system as a whole.

In addition to PAHs, straight-chain *n*-alkanes are useful as diagnostic markers of hydrocarbon sources (Charriau et al. 2009). The prominent presence of odd, long-chain alkanes in sediment reflects the major input of terrestrial sources in this shallow system through vascular plants (e.g., Meyers and Ishiwatari 1993; Harvey et al. 2014). Terrigenous aquatic (TAR) values can be useful to gauge the input of natural plant alkanes and were calculated for all sediment samples using Eq. 1 (Bourbonniere and Meyers 1996).

$$\text{TAR} = \frac{C_{27} + C_{29} + C_{31}}{C_{15} + C_{17} + C_{19}} \quad (1)$$

Calculated TAR values ranged from 0.97 to 11.40 with all stations other than site 5 having a TAR value > 1. This suggests terrestrial higher plant material as the predominant source (Bourbonniere and Meyers 1996) (supplemental tables S4 (A), (B), (C), and (D)). The elevated TAR values along with the trend of longer chain lengths and higher total concentrations in shallow sampling locations support the important role of direct runoff as a major input to this system. Total alkane concentration for the Lafayette River appears intermediate versus similar metropolitan rivers, with the Lafayette (4.68–40.83  $\mu\text{g g}^{-1}$  dry wt.) similar in concentration to the Scheldt River Basin, France (2.8–29  $\mu\text{g g}^{-1}$  dry wt.) (Charriau et al. 2009), and somewhat higher than that observed in the urban Shinano River in Japan (0.16–3.53  $\mu\text{g g}^{-1}$  dry wt.) (Hori et al. 2009).

### Hydrocarbon burden on invertebrates

Benthic inhabitants have often been used to gauge the impact of hydrocarbons on estuarine systems, particularly for those consumed (e.g. Burns and Teal 1979; Marcus and Stokes 1985; Gaspare et al. 2009; Li et al. 2021; Han et al. 2022). For the Lafayette, oyster tissues were lower than previous analysis of native oysters in 2011 (VA Dept. of Health 2012) with a present total PAH concentration of 561.2  $\text{ng g}^{-1}$  dry wt. compared to the 2011 value of 685.6  $\text{ng g}^{-1}$  dry wt. (VA Dept. of Health 2012). We did observe, however, a higher concentration of benzo(a)pyrene which is considered a probable human carcinogen and of concern (VA Dept. of Health 2012). The general trend for the oyster tissues was to favor

parent and HMW compounds indicating pyrogenic sources. A comparison of site 2 sediments in 2021 and the oyster tissues shows a good correspondence between major PAHs in both (Fig. 5). These include high relative abundances for Fl, Chr, Bbf, Bkf, and Ind. Some of these PAHs are also seen at high abundances when looking at the distribution of the HMW portion of lump coal including Fl, Chr, and Bbf (Fig. 4a). This implies oysters are exposed and accumulate similar PAHs that impact the sediment. This might be expected for the filter feeding oyster due to the known link between sediment contamination levels and bioaccumulation of PAHs in benthic organisms (Mitra et al. 2000).

In contrast, for blue crab tissues, the fact that few PAHs were found in tissues demonstrates crab's metabolic capabilities for hydrocarbon depuration (Singer and Lee 1977). The ability of invertebrates to metabolize hydrocarbons through the use of Phase I and II biotransformation enzymes is well known and may explain the lack of pattern among the PAHs detected along with the poor correlation to the closest surface sediment sampled for blue crabs (Livingstone 1998). Phase I involves the transformation of PAHs to phenols, quinones, and diol epoxides through the use of enzymes including cytochrome P450, epoxide hydrolases, and NAD(P)H quinone oxidoreductases (Livingstone 1998; Zacchi et al. 2019). Some of these metabolites can be excreted from the cell and are carcinogenic; thus, phase II enzymes including glutathione S-transferases and sulfotransferases are utilized to improve the metabolites solubility in water for depuration (Zacchi et al. 2019). Although values seen for both oysters and blue crabs are low, it demonstrates that PAHs and alkane hydrocarbons deposited to the system are being transferred to benthic inhabitants and further monitoring is warranted.

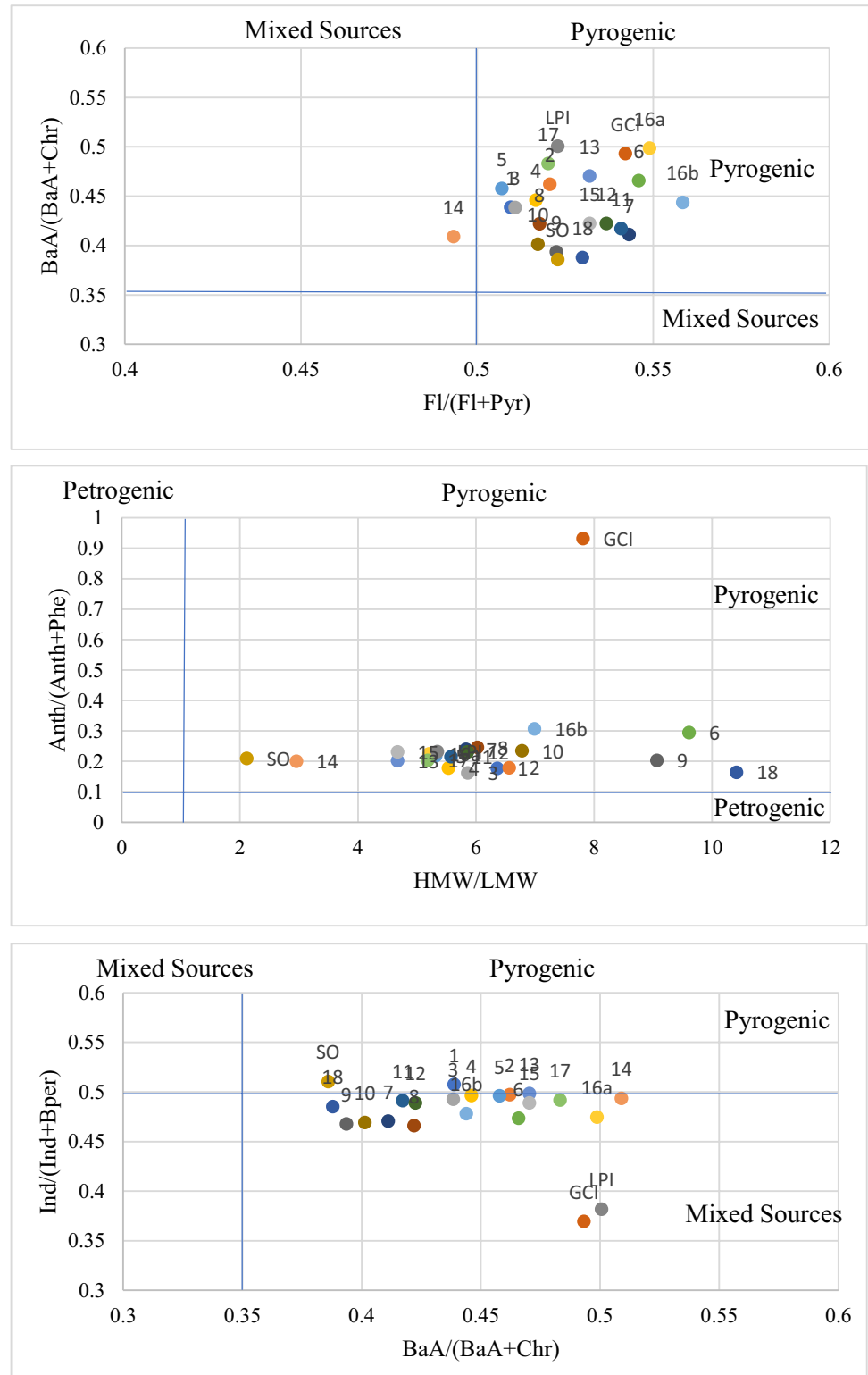
### Source assessment of PAHs to the Lafayette

While PAH concentrations in the Lafayette appear comparable to other metropolitan cities, an important issue is contributors to the system. In this shallow system with substantial drainage, both natural and anthropogenic sources are expected and provide structural PAH fingerprints that can allow major sources to be distinguished. To evaluate the potential sources of PAHs into the river sediment, two approaches were used. The first was the use of several diagnostic PAH ratios which have proven to be valuable across many environments (Yunker et al 2002; Moon et al. 2006; Rocha et al. 2017). These include HMW/LMW (Hwang and Foster 2006), Fl/(Fl + Pyr) (Rocha et al. 2017), phenanthrene/anthracene (Thavamani et al. 2012 and Yunker et al. 2002), Fl/Pyr (Thavamani et al. 2012 and Yunker et al. 2002), indeno[1,2,3-cd]pyrene/(indeno[1,2,3-cd]pyrene + benzo[g,h,i]perylene) (Rocha et al. 2017), benz[a]anthracene/(benz[a]anthracene + Chr) (Rocha et al. 2017), and anthracene/(anthracene + phenanthrene) (Rocha et al.

2017). Results for these calculated ratios are shown in supplemental table S6 and plotted in Fig. 6 showing a pattern consistent with pyrogenic and/or mixed sources as major PAH contributors to the system for all sediment samples depending on the ratio utilized. The large abundance of

HMW PAHs has been previously noted to represent pyrogenic sources for the nearby Chesapeake Bay (Kimbrough and Dickhut 2006), an argument also made for the dominance of parent PAHs seen in sediments (Zakaria et al. 2002). In contrast, the varied PAH distribution seen in

**Fig. 6** Source analysis plots utilizing PAH diagnostic ratio comparisons for the surface sediment samples. PAHs utilized include fluoranthene (Fl), pyrene (Pyr), phenanthrene (Phe), anthracene (Anth), indeno[1,2,3-cd]pyrene (Ind), benzo[g,h,i]perylene (Bper), benz[a]anthracene (BaA), and chrysene (Chr)



atmospheric deposition samples were less defined and suggested origins beyond pyrogenic sources alone can contribute through atmospheric transport (see supplemental table S6).

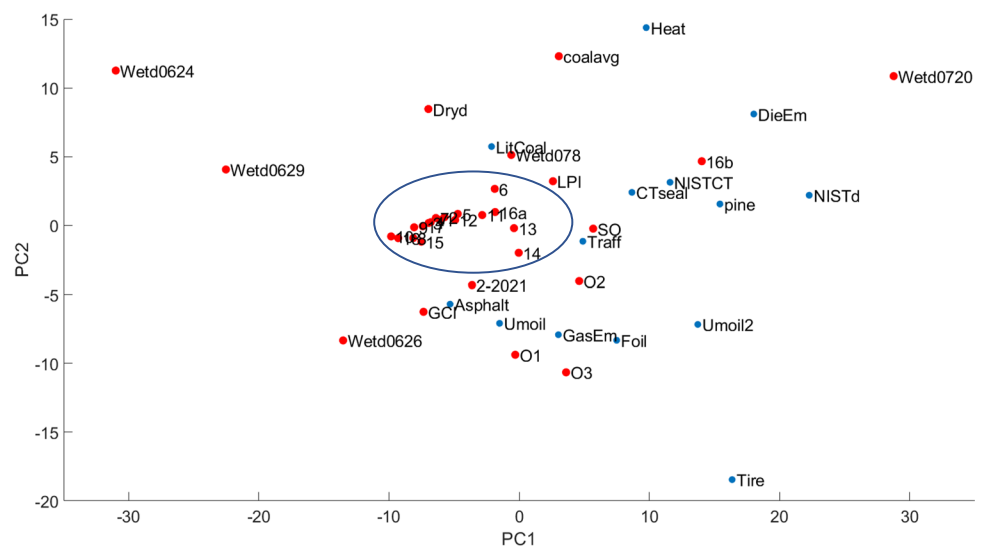
PAHs present in intact coals complicate the simple ratios often used for source assignments. In fact, the observed ratios suggested that the lump coal samples could be assigned as representing multiple sources rather than expected petrogenic sources alone (see supplemental table S6). The solid lump coal samples did not agree for the Phen and Anth ratio along with the multiple ratios examined showing contradicting pyrogenic, petrogenic, and mixed sources. These results suggest that the ratios utilized for source assignment are more nuanced and not universal. The observation from atmospheric deposition samples that transported coal dust was absent several low molecular weight PAHs suggests coal dust from lump (uncombusted) coal represents a potential source of PAHs to the system that mimics pyrogenic source(s). To account for multiple types of coal transported through the Lafayette watershed and inconsistencies in the ratio analysis, a more comprehensive set of measures is needed. An expanded suite of PAHs present in lump coals plus literature values were thus evaluated by PCA analysis as a second approach to better define the potential for lump coal dust as a significant source to sediments.

PCA examined the relationships among sediments versus 13 potential metropolitan PAH sources. The evaluation relied on those PAHs present across all potential contributions which narrowed the suite to 10 HMW PAHs found in all literature sources. Those major sources examined included residential heating (Heat) (Li et al. 2003), coal combustion (LitCoal) (Li et al. 2003), diesel vehicle particulate emissions (DieEm) (Li et al. 2003), gasoline vehicle particulate emissions (GasEm) (Li et al. 2003), traffic averages (Traff) (Li et al. 2003), used motor oil (Umoil

and Umoil2) (Wang et al. 2000 and Boonyatumanond et al. 2007), tire particles (Tire) (Boonyatumanond et al. 2007), NIST diesel particles (NISTd) (NIST standard reference material 1650a), asphalt (asphalt) (Boonyatumanond et al. 2007), fuel–oil combustion particles (Foil) (Li et al. 1999), pine-wood soot particles (pine) (Schauer et al. 2001), NIST coal tar (NISTCT) (NIST standard reference material 1597), coal tar sealant products (CTseal) (Mahler et al. 2005), and lump coal (coalavg). Results of the PCA analysis, including sediment samples, air deposition samples, oyster tissue samples, and numerous potential sources, found the first two principal components accounted for 68% of the variance between samples (Fig. 7). The loading plot for the first two principal components showed sediment closely aligned for PC1 and PC2 with potential sources of varied distance from the sediment cluster (Fig. 7). When assessing the varimax rotated loading scores for PC1, F1 was the largest contributing component in the positive direction with a loading score of 0.90, while the negative direction was numerous smaller contributions. For PC2, Bbf was the largest contributing component in the positive direction with a loading score of 0.66, while Bper, with a loading score of  $-0.63$ , was the largest contributor in the negative direction. Loading scores are shown in supplemental table S7 for the first 3 principal components.

Both of the lump coals analyzed here and literature coal combustion values showed a higher PC2 loadings due to elevated values of Bbf and lower values of Bper compared to sediment. The sediment samples have an increased value of Bper from known sources including gasoline particle emission, asphalt, and used motor oil which drive them in the negative direction for PC2. These common metropolitan sources also decrease the abundance of Bbf, driving the sediment samples in the negative direction for PC2. As a result, the sediment samples generally align between the

**Fig. 7** PCA loading scores plot of the first two principal components comparing the relative abundance of 10 HMW PAHs in sediments (1 through 18, LPI, GCI, SO, and 2–2021), wet deposition samples (Wetd0624, Wetd0626, Wetd0629, Wetd078, and Wetd0720), dry deposition (Dryd), average lump coal samples (coalavg), and oyster tissue samples (O1, O2, and O3) together with a variety of metropolitan sources. Blue circle includes all Lafayette sediment samples except 16b. Blue data points indicate literature sources, while red data points indicate data collected in this study



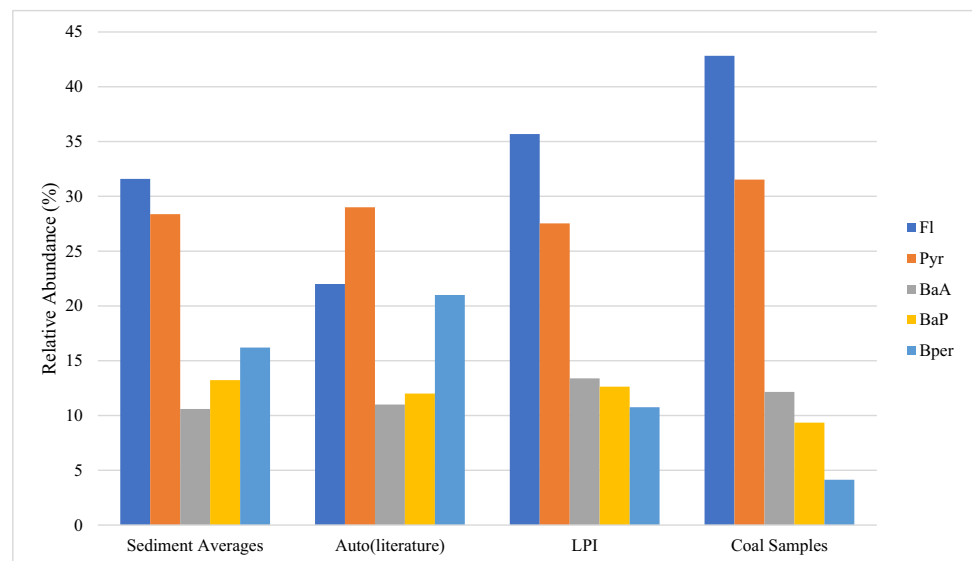
coal combustion and lump coal samples, dry deposition sample, and several automotive sources on the plot which reflect the mixed contributions (Fig. 7). The central position of the sediments in comparison to the coal combustion, lump coal, and various automotive sources reflects the influence from each source on the PAH distribution. With no known sources of coal combustion in proximity to the river, it appears that that lump coal dust carried by direct deposition plus automotive sources are important contributors. Large differences between the sediment and diesel sources were observed, indicating diesel particulate emission and diesel are not major contributors to most surface sediments. Sediments at Site 16b appears to be an outlier and showed an influence from diesel sources and likely due to its proximity to a major thoroughfare for truck transport (Hampton Blvd—Fig. 1). An important observation from the PCA analysis was that multiple sources were present in air deposition samples being transported to the watershed. The dry deposition sample agrees well with the sediment in the first component while being driven in the positive direction for PC2. This puts the dry deposition samples of transported coal dust in close proximity to literature distributions seen for coal combustion samples. The absence of coal combustion in proximity to atmospheric sample collections argues that lump coal dust which has lost LMW PAHs is the major source and mimics combustion products routinely encountered as aerosols. It suggests that for this system, lump coal dust acts as a unique source of PAHs which ultimately are sequestered in river sediments and direct deposition is the major pathway.

When evaluating samples collected in this study, the relative abundance distribution for the HMW PAHs in the Lafayette River surface sediment shown in Fig. 4c showed high concentrations of Fl, Pyr, Chr, and Bbf, which are also seen

in the HMW PAH distribution for lump coal and dry atmospheric deposition (Fig. 4a and b). This suggests that lump coal dust is being transported through the atmospheric particles to the watershed. Lafayette sediments also had higher abundances of benzo[k]fluoranthene (Bkf), Bper, and Ind than in lump coal. These higher abundances support several automotive sources as additional source of PAHs impacting Lafayette surface sediment. These PAH compounds have been linked to automotive sources impact on the atmosphere and used as tracers of automotive emissions (Miguel and Pereira 1989). The Lafayette surface sediment samples had much lower abundances of LMW PAHs than the lump coal samples. These PAHs were major compounds in the coal sample indicating LMW PAHs in coal are not being transported through atmospheric deposition or settling into the sediment. This could be due to PAH weathering events as well as LMW PAHs favoring the vapor phase over the particulate phase during summer months (Abdel-Shafy and Mansour 2016).

To better assess the impact of lump coal dust and automotive sources on PAHs transported to the Lafayette system, the relative abundance of Fl, Pyr, BaA, benzo[a]pyrene (BaP), and Bper were compared with literature values and collected lump coal samples (Fig. 8). As most of the Lafayette River sediment seems to have similar sources, the average for all stations was utilized. Lafayette sediments show good agreement with input of automotive sources in addition to an influence from lump coal dust. The Fl value is higher than automotive while Bper is lower than the automotive sources, indicating the input of lump coal dust into the system. Site LPI, which is located adjacent to the coal terminal, reinforces this suggestion as it had a similar distribution to lump coal sources. These results support the contention that lump coal dust is a major source of PAHs to the Lafayette

**Fig. 8** The relative abundance of several diagnostic HMW PAHs in sediments compared to likely sources for the region. Auto sources are inclusive of gasoline (Alsberg et al. 1985; Rogge et al. 1993a; Singh et al. 1993; Khalili et al. 1995), diesel (Rogge et al. 1993a; Khalili et al. 1995), tunnel air (Colmsjö et al. 1986; Benner et al. 1989; Khalili et al. 1995), and road debris (Rogge et al. 1993b; Singh et al. 1993). Coal is represented by samples collected in this study. Sediment averages comprise all Lafayette sediment samples collected in 2014



surface sediments, in addition to the expected significant input from a variety of automotive sources in this metropolitan environment.

Coal is exported near the Lafayette system through a dockside coal terminal that has operated for over a century (Fig. 1). While the specific type of coal was not determined, PAH concentrations and distributions are known to vary among coal types (Gao et al. 2019) and the concentrations obtained are certainly within the range often observed (Gao et al. 2019). The similarity seen for the dry atmospheric deposition sample and HMW PAHs for coal in particular point to atmospheric transport of lump coal dust as a major route for input to the Lafayette. The limited suite of LMW PAHs present in the dry deposition sample also implies the LMW PAHs found in coal remain in the vapor phase while HMW PAHs are in the particulate phase and undergo dry atmospheric deposition (Chimjarn et al. 2021). The variability in wet deposition suggests additional sources are also being transported during rain events.

Non-point sources are known to transport PAHs and other contaminants from rainfall or irrigation which mobilizes pollutants as runoff and through groundwaters (Hoffman et al. 1984). Near shore runoff appears to be an important element based on PAHs' higher concentrations in shallower locations. As the metropolitan watershed itself is large (43.28 km<sup>2</sup>) (Egerton et al. 2014), there is adequate opportunity for surface-adsorbed PAHs to be transported during storm events with concentration elevated in shallow shoreline regions. These shallow regions also have higher TOC which correlates to higher PAH concentrations likely due to the PAHs being retained in sediment with more TOC at a higher rate and remaining adsorbed to the particles. The deeper central channel is also subject to more sediment transport affecting accumulation over time.

Both ratio and PCA source analysis techniques provided valuable insight into the origin of the PAHs impacting the Lafayette surface sediment. Both approaches show the presence of lump coal dust impacting the sediment together with several potential automotive sources including gasoline particle emission, asphalt, and used motor oil. PCA analysis provided more detailed insight into specific sources and identified the importance of atmospheric transport of lump coal dust to PAHs present in sediments.

## Conclusion

Previous work has shown the dominant source of PAHs to the heavily impacted nearby Elizabeth River sediment to be creosote and coal combustion (Walker and Dickhut 2001) with automotive sources as an input through atmospheric deposition for the Southern Chesapeake Bay region (Dickhut et al. 2000). The Lafayette River and its large metropolitan

watershed show similar influences, with adjacent deposition samples validating the impact of atmospheric transport for materials directly to the river as well as drainage for residential areas and runoff. It is apparent, however, that either directly through deposition or indirectly through runoff, transported lump coal dust rather than combusted products together with automotive sources are important contributors to the PAHs present in the Lafayette River. The *n*-alkanes in the system indicate natural terrestrial sources are also important contributors through runoff. The Lafayette River system's total *n*-alkane and PAH concentration in surface sediment is at reasonable levels when compared to other industrial systems. The benthic inhabitants reflect accumulation of PAHs in tissue as well as metabolic capabilities of crabs. These results provide a baseline to evaluate ongoing restoration efforts for the Lafayette including introduction of wetlands, constructions of rain gardens, and nearshore oyster reefs.

**Supplementary Information** The online version contains supplementary material available at <https://doi.org/10.1007/s11356-023-25563-y>.

**Acknowledgements** We thank Pete Sedwick for assistance with air deposition sampling. Special thanks to Carrie Fleiger and Shelby Coleman for their contributions to collection and processing of samples for GC/MS analysis and Karen Taylor for laboratory oversight.

**Author contribution** Nathaniel Maynard will act as the corresponding author. For this manuscript, NM led sample collection and analysis efforts, major data analysis/interpretation, and writing. HRH contributed to sample collection, lab support, and writing/editing of the manuscript.

**Funding** This project was funded by the National Science Foundation REU program and Chemical Oceanography program awards to HRH (OCE1659543 and OCE1636045) and the department of Ocean and Earth Sciences at Old Dominion University (Dorothy Brown Smith Scholarship) to NM.

**Data availability** The datasets generated during the current study are available from the corresponding author upon request.

## Declarations

**Ethics approval** Not applicable

**Consent to participate** Not applicable

**Consent to publish** Not applicable

**Competing interests** The authors declare that they have no known conflict of interest (financial or non-financial) or personal relationships that could have appeared to influence the work reported in this paper.

## References

Abdel-Shafy HI, Mansour MSM (2016) A review on polycyclic aromatic hydrocarbons: source, environmental impact, effect on

- human health and remediation. *Egypt J Pet* 25(1):107–123. <https://doi.org/10.1016/j.ejpe.2015.03.011>
- Alsberg TE, Sternberg U, Westerholm RN, Strandell ME, Rannug U, Sundvall A, Romert L, Bernson V, Pettersson B et al (1985) Chemical and biological characterization of organic material from gasoline exhaust particles. *Environ Sci Technol* 19:43–50. <https://doi.org/10.1021/es00131a003>
- Benner BA Jr, Gordon GE, Wise SA (1989) Mobile sources of atmospheric polycyclic aromatic hydrocarbons: a roadway tunnel study. *Environ Sci Technol* 23:1269–1278. <https://doi.org/10.1021/es00068a014>
- Blair CH, Cox JH, Kuo CY (1976) Investigation of flushing time in the Lafayette River, Norfolk, Virginia; School of Engineering Technical Report No. 76-C4; Old Dominion University: Norfolk, VA, USA
- Boonyatumanond R, Murakami M, Wattayakorn G, Togo A, Takada H (2007) Sources of polycyclic aromatic hydrocarbons (PAHs) in street dust in a tropical Asian mega-city, Bangkok, Thailand. *Sci Total Environ* 384:420–432. <https://doi.org/10.1016/j.scitotenv.2007.06.046>
- Bounds WJ, Johannesson KH (2007) Arsenic addition to soils from airborne coal dust originating at a major coal shipping terminal. *Water Air Soil Pollution* 185:195–207. <https://doi.org/10.1007/s11270-007-9442-9>
- Burns KA, Teal JM (1979) The West Falmouth oil spill: hydrocarbons in the salt marsh ecosystem. *Est Coast Mar Sci* 8:349–360. [https://doi.org/10.1016/0302-3524\(79\)90052-5](https://doi.org/10.1016/0302-3524(79)90052-5)
- Bourbonniere RA, Meyers PA (1996) Sedimentary geolipid records of historical changes in the watersheds and productivities of Lakes Ontario and Erie. *Limnol Oceanogr* 41:352–359. <https://doi.org/10.4319/lo.1996.41.2.0352>
- Charriau A, Bodineau L, Ouddane B, Fischer JC (2009) Polycyclic aromatic hydrocarbons and *n*-alkanes in sediments of the Upper Scheldt River Basin: contamination levels and source apportionment. *J Environ Monit* 11:1086–1093. <https://doi.org/10.1039/B819928K>
- Chauhan A, Fazlurrahman, Oakeshott JG, Jain RK (2008) Bacterial metabolism of polycyclic aromatic hydrocarbons: strategies for bioremediation. *Indian J Microbiol* 48(1):95–113. <https://doi.org/10.1007/s12088-008-0010-9>
- Chimjarn S, Delhomme O, Millet M (2021) Temporal distribution and gas/particle partitioning of polycyclic aromatic hydrocarbons (PAHs) in the atmosphere of Strasbourg, France. *Atmosphere* 12(3):337. <https://doi.org/10.3390/atmos12030337>
- Colmsjö AL, Zebühr YU, Östman CE, Wådding Å, Söderström H (1986) Polynuclear aromatic compounds in the ambient air of Stockholm. *Chemosphere* 15:162–182. [https://doi.org/10.1016/0045-6535\(86\)90569-2](https://doi.org/10.1016/0045-6535(86)90569-2)
- Davis E, Walker TR, Adams M, Willis R, Norris GA, Henry RC (2019) Source apportionment of polycyclic aromatic hydrocarbons (PAHs) in small craft harbor (SCH) surficial sediments in Nova Scotia, Canada. *Sci Total Environ* 691:528–537. <https://doi.org/10.1016/j.scitotenv.2019.07.114>
- Dickhut R, Canuel E, Gustafson K, Liu K, Arzayus K, Walker S, Edgcombe G, Gaylor M, MacDonald E (2000) Automotive sources of carcinogenic polycyclic aromatic hydrocarbons associated with particulate matter in the Chesapeake Bay region. *Environ Sci Technol* 34(21):4635–4640. <https://doi.org/10.1021/es000971e>
- Egerton TA, Morse RE, Marshall HG, Mulholland MR (2014) Emergence of algal blooms: the effects of short-term variability in water quality on phytoplankton abundance, diversity, and community composition in a tidal estuary. *Microorganisms* 2:33–57. <https://doi.org/10.3390/microorganisms2010033>
- Gao B, Feng Q, Zhou L, Wu H, Alam E (2019) Distributions of polycyclic aromatic hydrocarbons in coal in China. *Pol J Environ Stud* 28(3):1665–1674. <https://doi.org/10.15244/pjoes/89899>
- Gaspere L, Machiwa JF, Mdachi SJM, Streck G, Brack W (2009) Polycyclic aromatic hydrocarbon (PAH) contamination of surface sediments and oysters from the inter-tidal areas of Dar es Salaam, Tanzania. *Environ Pollut* 157:24–34. <https://doi.org/10.1016/j.envpol.2008.08.002>
- Han M, Liu F, Kang Y, Zhang R, Yu K, Wang Y, Wang R (2022) Occurrence, distribution, sources, and bioaccumulation of polycyclic aromatic hydrocarbons (PAHs) in multi environmental media in estuaries and the coast of the Beibu Gulf, China: a health risk assessment through seafood consumption. *Environ Sci Pollut Res* 29:52493–52506. <https://doi.org/10.1007/s11356-022-19542-y>
- Hatzinger PB, Alexander M (1995) Effect of aging of chemicals in soil on their biodegradability and extractability. *Environ Sci Technol* 29(2):537–545. <https://doi.org/10.1021/es00002a033>
- Hartzell SE, Unger MA, McGee BL, Wilson SM, Yonkos LT (2017) Effects-based spatial assessment of contaminated estuarine sediments from Bear Creek, Baltimore Harbor, MD, USA. *Environ Sci Pollut Res* 24:22158–22172. <https://doi.org/10.1007/s11356-017-9667-0>
- Harvey HR, Taylor KA, Pie HV, Mitchelmore CL (2014) Polycyclic aromatic and aliphatic hydrocarbons in Cchukchi sea biota and sediments and their toxicological response in the arctic cod, *Boreogadus saida*. *Deep Sea Res Part II* 102:32–55. <https://doi.org/10.1016/j.dsr2.2013.07.013>
- Hoffman EJ, Mills GL, Latimer JS, Quinn JG (1984) Urban runoff as a source of polycyclic aromatic hydrocarbons to coastal waters. *Environ Sci Technol* 18(8):580–587. <https://doi.org/10.1021/es00126a003>
- Hori T, Shiota N, Asada T, Oikawa K, Kawata K (2009) Distribution of polycyclic aromatic hydrocarbons and *n*-alkanes in surface sediments from Shinano River, Japan. *Bull Environ Contam Toxicol* 83:455–461. <https://doi.org/10.1007/s00128-009-9743-3>
- Hwang HM, Foster GD (2006) Characterization of polycyclic aromatic hydrocarbons in urban stormwater runoff flowing into the tidal Anacostia River, Washington, DC, USA. *Environ Pollut* 140(3):416–426. <https://doi.org/10.1016/j.envpol.2005.08.003>
- Javier Rivas F (2006) Polycyclic aromatic hydrocarbons sorbed on soils: a short review of chemical oxidation based treatments. *J Hazard Mater* 138(2):234–251. <https://doi.org/10.1016/j.jhazmat.2006.07.048>
- Khalili NR, Sceff PA, Holsen TM (1995) PAH source fingerprints for coke ovens, diesel and gasoline engines, highway tunnels, and wood combustion emissions. *Atmos Environ* 29:533–542. [https://doi.org/10.1016/1352-2310\(94\)00275-P](https://doi.org/10.1016/1352-2310(94)00275-P)
- Kim SJ, Kweon O, Jones RC, Freeman JP, Edmondson RD, Cerniglia CE (2007) Complete and integrated pyrene degradation pathway in *Mycobacterium vanbaalenii* PYR-1 based on systems biology. *J Bacteriol* 189(2):464–472. <https://doi.org/10.1128/JB.01310-06>
- Kimbrough KL, Dickhut RM (2006) Assessment of polycyclic aromatic hydrocarbon input to urban wetlands in relation to adjacent land use. *Mar Pollut Bull* 52(11):1355–1363. <https://doi.org/10.1016/j.marpolbul.2006.03.022>
- Kleinosky LR, Yarnal B, Fisher A (2007) Vulnerability of hampton roads, Virginia to storm-surge flooding and sea-level rise. *Nat Hazards* 40:43–70. <https://doi.org/10.1007/s11069-006-0004-z>
- Korfmacher WA, Wehry EL, Mamantov G, Natusch DFS (1980) Resistance to photochemical decomposition of polycyclic aromatic hydrocarbons vapor-adsorbed on coal fly ash. *Environ Sci Technol* 14(9):1094–1099. <https://doi.org/10.1021/es00169a019>
- Li A, Jang JK, Scheff PA (2003) Application of EPA CMB8.2 model for source apportionment of sediment PAHs in Lake Calumet, Chicago. *Environ Sci Technol* 37:2958–2965. <https://doi.org/10.1021/es026309v>
- Li CT, Mi HH, Lee WJ, You WC, Wang YF (1999) PAH emission from the industrial boilers. *J Hazard Mater A69*:1–11. [https://doi.org/10.1016/s0304-3894\(99\)00097-7](https://doi.org/10.1016/s0304-3894(99)00097-7)

- Li Y, Lu G, Wang WX, Li H, You J (2021) Temporal and spatial characteristics of PAHs in oysters from the Peral River Estuary, China during 2015–2020. *Sci Total Environ* 793:148495. <https://doi.org/10.1016/j.scitotenv.2021.148495>
- Livingstone DR (1998) The fate of organic xenobiotics in aquatic ecosystems: quantitative and qualitative differences in biotransformation by invertebrates and fish. *Comp Biochem Physiol a: Mol Integr Physiol* 120(1):43–49. [https://doi.org/10.1016/S1095-6433\(98\)10008-9](https://doi.org/10.1016/S1095-6433(98)10008-9)
- Macias-Tapia A, Mulholland MR, Selden CR, Loftis JD, Bernhardt PW (2021) Effects of tidal flooding on estuarine biogeochemistry: quantifying flood-driven nitrogen inputs in an urban, lower Chesapeake Bay sub-tributary. *Water Res* 201:117329. <https://doi.org/10.1016/j.watres.2021.117329>
- Mahler BJ, Van Metre PC, Bashara TJ, Wilson JT, Johns DA (2005) Parking lot sealcoat: an unrecognized source of urban PAHs. *Environ Sci Technol* 39(15):5560–5566. <https://doi.org/10.1021/es0501565>
- Marcus JM, Stokes TP (1985) Polynuclear aromatic hydrocarbons in oyster tissue around three coastal marinas. *Bull Environ Contam Toxicol* 35:835–844. <https://doi.org/10.1007/BF01636595>
- Masoner JR, Kolpin DW, Cozzarelli IM, Barber LB, Burden DS, Foreman WT, . . . Bradley PM (2019) Urban stormwater: an overlooked pathway of extensive mixed contaminants to surface and groundwaters in the United States. *Environ Sci Technol* 53(17):10070–10081. <https://doi.org/10.1021/acs.est.9b02867>
- Masood N, Zakaria MP, Halimoon N, Aris AZ, Magam SM, Kannan N, Mustafa S, Ali MM, Keshavarzifard M, Vaezzadeh V, Alkhadher SAA (2016) Anthropogenic waste indicators (AWIs), particularly PAHs and LABs, in Malaysian sediments: application of aquatic environment for identifying anthropogenic pollution. *Mar Pollut Bull* 102(1):160–175. <https://doi.org/10.1016/j.marpolbul.2015.11.032>
- Meyers PA, Ishiwatari R (1993) Lacustrine organic geochemistry: an overview of indicators of organic matter sources and diagenesis in lake sediments. *Org Geochem* 20:867–900. [https://doi.org/10.1016/0146-6380\(93\)90100-P](https://doi.org/10.1016/0146-6380(93)90100-P)
- Miguel AH, Pereira PAP (1989) Benzo(k)fluoranthene, Benzo(ghi)perylene, and Indeno(1,2,3-cd)pyrene: new tracers of automotive emissions in receptor modeling. *Aerosol Sci Technol* 10(2):292–295. <https://doi.org/10.1080/02786828908959265>
- Mitra S, Klerks PL, Bianchi TS, Means J, Carman KR (2000) Effects of estuarine organic matter biogeochemistry on the bioaccumulation of PAHs by two epibenthic species. *Estuaries* 23:864–876. <https://doi.org/10.2307/1353003>
- Moon HB, Kannan K, Lee SJ, Ok G (2006) Atmospheric deposition of polycyclic aromatic hydrocarbons in an urban and a suburban area of Korea from 2002 to 2004. *Arch Environ Contam Toxicol* 51:494–502. <https://doi.org/10.1007/s00244-006-0002-x>
- Mothershead RF, Hale RC, Greaves J (1991) Xenobiotic compounds in blue crabs from a highly contaminated urban subestuary. *Environ Toxicol Chem* 10(10):1341–1349. <https://doi.org/10.1002/etc.5620101013>
- Mulholland MR, Morse R, Egerton T, Bernhardt PW, Filippino KC (2018) Blooms of dinoflagellate mixotrophs in a lower Chesapeake Bay tributary: carbon and nitrogen uptake over diurnal, seasonal, and interannual timescales. *Estuaries Coasts* 41:1744–1765. <https://doi.org/10.1007/s12237-018-0388-5>
- Neff JM, Stout SA, Gunster DG (2005) Ecological risk assessment of polycyclic aromatic hydrocarbons in sediments: identifying sources and ecological hazard. *Integr Environ Assess Manag* 1(1):22–33. [https://doi.org/10.1897/IEAM\\_2004a-016.1](https://doi.org/10.1897/IEAM_2004a-016.1)
- Nemr AE, Moneer AA, Ragab S, Sikaily AE (2016) Distribution and sources of n-alkanes and polycyclic aromatic hydrocarbons in shellfish of the Egyptian Red Sea coast. *Egypt J Aquat Res* 42(2):121–131. <https://doi.org/10.1016/j.ejar.2016.05.003>
- NIST standard reference material (1597) Complex Mixture of Polycyclic Aromatic Hydrocarbons from Coal Tar 2006. National Institute of Standards and Technology. Retrieved from [https://srms.nist.gov/certificates/view\\_cert2gif.cfm?certificate=1597](https://srms.nist.gov/certificates/view_cert2gif.cfm?certificate=1597). Accessed 26 June 2022
- NIST standard reference material (1650a). Diesel Particulate Matter 2006. National Institute of Standards and Technology.
- NIST standard reference material (1944) New York/New Jersey waterway sediment. National Institute of Standards and Technology
- NOAA (2020) Maryland oyster restoration update: progress toward the Chesapeake Bay watershed agreement's 'Ten Tributaries by 2025' oyster sub-outcome. (2021). Retrieved from [https://www.chesapeakebay.net/documents/2020\\_Virginia\\_Oyster\\_Restoration\\_Update\\_FINAL.pdf](https://www.chesapeakebay.net/documents/2020_Virginia_Oyster_Restoration_Update_FINAL.pdf). Accessed 12 April 2022
- Norris G, Henry R (2019) Unmix optimum analysis of PAH sediment sources. *Sci Total Environ* 673:831–838. <https://doi.org/10.1016/j.scitotenv.2019.03.227>
- Pereira WE, Hostettler FD, Rapp JB (1996) Distribution and fate of chlorinated pesticides, biomarkers and polycyclic aromatic hydrocarbons in sediments along a contamination gradient from a point-source in San Francisco Bay, California. *Mar Environ Res* 41:299–314. [https://doi.org/10.1016/0141-1136\(95\)00021-6](https://doi.org/10.1016/0141-1136(95)00021-6)
- Pies C, Hoffmann B, Petrowsky J, Yang Y, Ternes TA, Hofmann T (2008) Characterization and source identification of polycyclic aromatic hydrocarbons (PAHs) in river bank soils. *Chemos* 72:1594–1601. <https://doi.org/10.1016/j.chemosphere.2008.04.021>
- Qiao M, Wang CX, Huang SB, Wang DH, Wang ZJ (2006) Composition, sources, and potential toxicological significance of PAHs in the surface sediments of the Meiliang Bay, Taihu Lake, China. *Environ Int* 32:28–33. <https://doi.org/10.1016/j.envint.2005.04.005>
- Rizzi J, Pérez-Albaladejo E, Fernandes D, Contreras J, Froehner S, Porte C (2017) Characterization of quality of sediments from Paranaguá Bay (Brazil) by combined in vitro bioassays and chemical analyses. *Environ Toxicol Chem* 36(7):1811–1819. <https://doi.org/10.1002/etc.3553>
- Rocha MJ, Dores-Sousa JL, Cruzeiro C, Rocha E (2017) PAHs in water and surface sediments from Douro River estuary and Porto Atlantic coast (Portugal)-impacts on human health. *Environ Monit Assess* 189(8):425. <https://doi.org/10.1007/s10661-017-6137-6>
- Rogge WF, Hildemann LM, Mazurek MA, Cass G (1993a) Sources of fine organic aerosol. 2. Noncatalyst and catalyst-equipped automobile and heavy-duty diesel trucks. *Environ Sci Technol* 27:636–651. <https://doi.org/10.1021/es00041a007>
- Rogge WF, Hildemann LM, Mazurek MA, Cass G, Simonelt BR (1993) Sources of fine organic aerosol: 3. Road dust, tire debris, and organometallic brake lining dust: roads as sources and sinks. *Environ Sci Technol* 27:1892–1904. <https://doi.org/10.1021/es00046a019>
- Saha M, Togo A, Mizukawa K, Murakami M, Takada H, Zakaria MP, Chiem NH, Tuyen BC, Prudente M, Boonyatumanond R (2009) Sources of sedimentary PAHs in tropical Asian waters: differentiation between pyrogenic and petrogenic sources by alkyl homolog abundance. *Mar Pollut Bull* 58:189–200. <https://doi.org/10.1016/j.marpolbul.2008.04.049>
- Schauer JJ, Kleeman MJ, Cass GR, Simoneit BRT (2001) Measurement of emissions from air pollution sources. 3. C1–C29 organic compounds from fireplace combustion of wood. *Environ Sci Technol* 35(9):1716–1728. <https://doi.org/10.1021/es001331e>
- Singer SC, Lee RF (1977) Mixed function oxygenase activity in blue crab, *Callinectes Sapidus*: tissue distribution and correlation with changes during molting and development. *Biol Bull* 153:377–386. <https://doi.org/10.2307/1540443>
- Singh AK, Gin MF, Ni F, Christensen ER (1993) A source-receptor method for determining non-point source of PAHs to the



- Milwaukee Harbor estuary. *Water Sci Technol* 28:91–102. <https://doi.org/10.2166/wst.1993.0607>
- Sofowote UM, McCarty BE, Marvin CH (2008) Source apportionment of PAH in Hamilton Harbour suspended sediments: comparison of two factor analysis methods. *Environ Sci Technol* 42:6007–6014. <https://doi.org/10.1021/es800219z>
- Thavamani P, Megharaj M, Naidu R (2012) Multivariate analysis of mixed contaminants (PAHs and heavy metals) at manufactured gas plant site soils. *Environ Monit Assess* 184(6):3875–3885. <https://doi.org/10.1007/s10661-011-2230-4>
- The City of Norfolk (2013) Norfolk City Council. *plaNorfolk2030: City of Norfolk Chesapeake Bay Preservation Area Program Supplement*, Mar. [www.norfolk.gov/1376/plaNorfolk2030](http://www.norfolk.gov/1376/plaNorfolk2030)
- Tolosa I, de Mora S, Sheikholeslami MR, Villeneuve J, Bartocci J, Cattini C (2004) Aliphatic and aromatic hydrocarbons in coastal Caspian Sea sediments. *Mar Pollut Bull* 48(1–2):44–60. [https://doi.org/10.1016/S0025-326X\(03\)00255-8](https://doi.org/10.1016/S0025-326X(03)00255-8)
- Virginia Department of Health (2012) Consumption advisory guidelines for oysters contaminated with polycyclic aromatic hydrocarbons. October 11, 2012. Retrieved from [https://www.vdh.virginia.gov/content/uploads/sites/12/2016/04/Norfolk\\_Lafayette-River-PAHs\\_10-11-2012.pdf](https://www.vdh.virginia.gov/content/uploads/sites/12/2016/04/Norfolk_Lafayette-River-PAHs_10-11-2012.pdf). Accessed 8 July 2022
- Vogelbein WK, Unger MA, Gauthier D (2008) The Elizabeth River monitoring program 2006–2007: association between mummichog liver histopathology and sediment chemical contamination. Virginia Institute of Marine Science, William & Mary. Retrieved from <https://scholarworks.wm.edu/reports/2534>. Accessed 12 April 2022
- Walker SE, Dickhut RM (2001) Sources of PAHs to sediments of the Elizabeth River, VA. *Soil Sediment Contam* 10:611–632. <https://doi.org/10.1080/20015891109464>
- Wang G, Huang L, Zhao X, Niu H, Dai Z (2006) Aliphatic and polycyclic aromatic hydrocarbons of atmospheric aerosols in five locations of Nanjing urban area, China. *Atmos Res* 81(1):54–66. <https://doi.org/10.1016/j.atmosres.2005.11.004>
- Wang J, Jia CR, Wong CK, Wong PK (2000) Characterization of polycyclic aromatic hydrocarbons created in lubricating oils. *Water Air Soil Pollut* 120:381–396. <https://doi.org/10.1023/A:1005251618062>
- Wang XC, Zhang YX, Robert FC (2001) Distribution and partitioning of polycyclic aromatic hydrocarbons (PAHs) in different size fractions in sediments from Boston Harbor, United States. *Mar Poll Bull* 42(11):1139–1149. [https://doi.org/10.1016/S0025-326X\(01\)00129-1](https://doi.org/10.1016/S0025-326X(01)00129-1)
- White EG (1972) A physical hydrographic study of the Lafayette River. M.S. Thesis, Norfolk, VA, USA: Old Dominion University
- Yim UH, Hong SH, Shim WJ, Oh JR, Chang M (2005) Spatio-temporal distribution and characteristics of PAHs in sediments from Masan Bay, Korea. *Mar Poll Bull* 50:319–326. <https://doi.org/10.1016/j.marpolbul.2004.11.003>
- Yunker MB, Macdonald RW, Vingarzan R, Mitchell RH, Goyette D, Sylvestre S (2002) PAHs in the Fraser River basin: a critical appraisal of PAH ratios as indicators of PAH sources and composition. *Org Geochem* 33:489–515. [https://doi.org/10.1016/S0146-6380\(02\)00002-5](https://doi.org/10.1016/S0146-6380(02)00002-5)
- Zacchi FL, Dos Reis IMM, Siebert MN, Mattos JJ, Flores-Nunes F, Toledo-Silva G, . . . Bainy ACD (2019) Differential responses in the biotransformation systems of the oyster *Crassostrea gasar* (Adanson, 1757) elicited by pyrene and fluorene: molecular, biochemical and histological approach - Part I. *Aquat Toxicol* 216: 105318. <https://doi.org/10.1016/j.aquatox.2019.105318>
- Zakaria MP, Takada H, Tsutsumi S, Ohno K, Yamada J, Kouno E, Kumata H (2002) Distribution of polycyclic aromatic hydrocarbons (PAHs) in rivers and estuaries in Malaysia: a widespread input of petrogenic PAHs. *Environ Sci Technol* 36(9):1907–1918. <https://doi.org/10.1021/es011278+>
- Zimmerman CF, Keefe CW, Bashe J (1997) Determination of carbon and nitrogen in sediments and particulates of estuarine/coastal waters using elemental analysis - method 440.0. U.S. Environmental Protection Agency, Cincinnati, OH

**Publisher's note** Springer Nature remains neutral with regard to jurisdictional claims in published maps and institutional affiliations.

Springer Nature or its licensor (e.g. a society or other partner) holds exclusive rights to this article under a publishing agreement with the author(s) or other rightsholder(s); author self-archiving of the accepted manuscript version of this article is solely governed by the terms of such publishing agreement and applicable law.